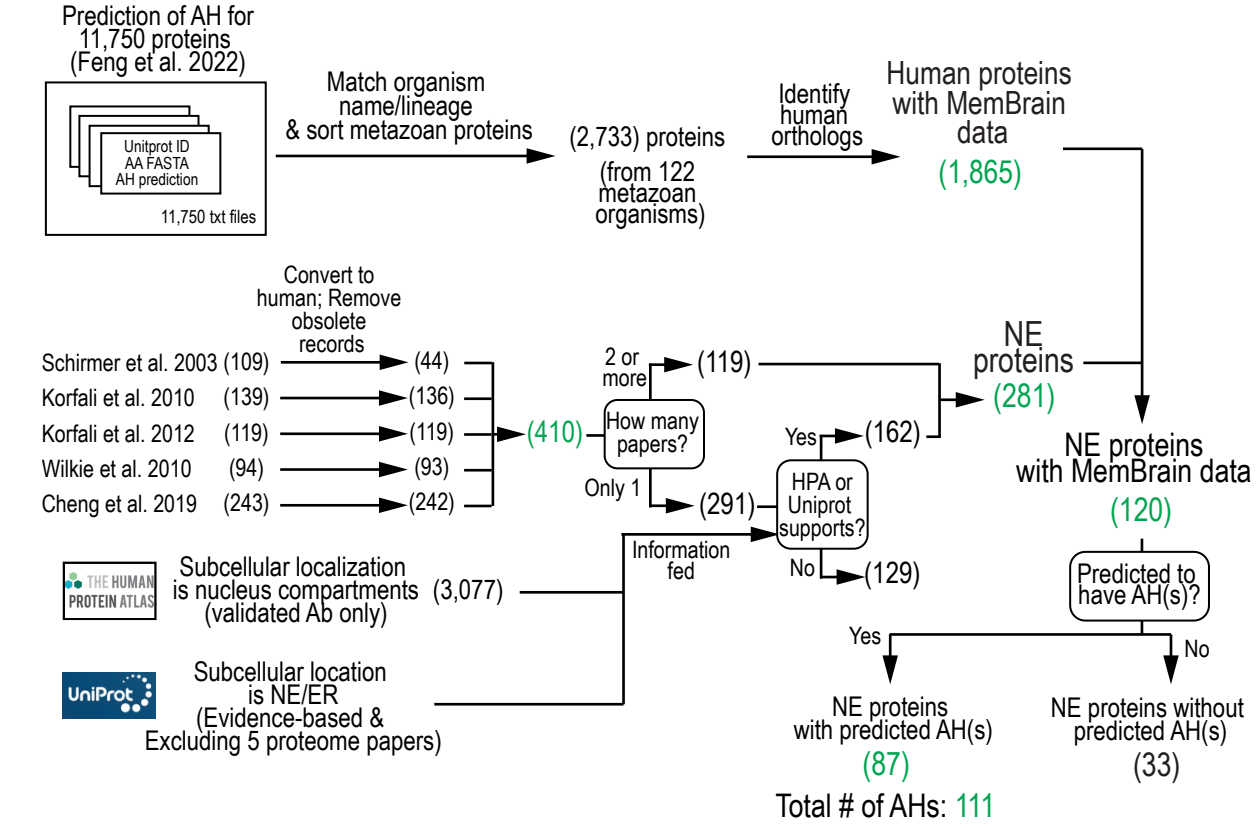
A
Prediction of AH for 11,750 proteins (Feng et al. 2022)
Unitprot ID
AA FASTA
AH prediction
11,750 txt files
Match organism name/lineage & sort metazoan proteins
(2,733) proteins (from 122 metazoan organisms)
Identify human orthologs
Human proteins with MemBrain data
(1,865)
Convert to human; Remove obsolete records
Schirmer et al. 2003 (109) (44)
Korfali et al. 2010 (139) (136)
Korfali et al. 2012 (119) (119)
Wilkie et al. 2010 (94) (93)
Cheng et al. 2019 (243) (242)
(410)
How many papers?
2 or more (119)
Only 1 (291)
NE proteins (281)
Yes (162)
HPA or Uniprot supports?
No (129)
Information fed
THE HUMAN PROTEIN ATLAS
Subcellular localization is nucleus compartments (validated Ab only) (3,077)
UniProt
Subcellular location is NE/ER (Evidence-based & Excluding 5 proteome papers)
NE proteins with MemBrain data
(120)
Predicted to have AH(s)?
Yes
No
NE proteins with predicted AH(s)
(87)
NE proteins without predicted AH(s)
(33)
Total # of AHs: 111

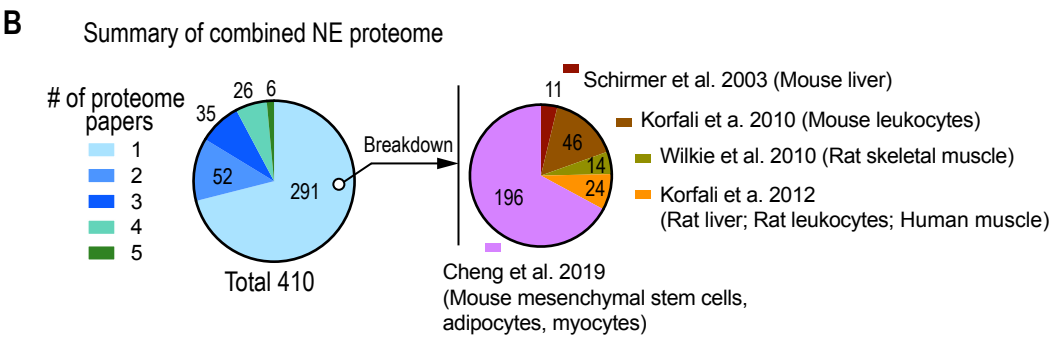
B
Summary of combined NE proteome
# of proteome papers
1
2
3
4
5
35
26
6
52
291
Total 410
Breakdown
11
46
14
24
196
Schirmer et al. 2003 (Mouse liver)
Korfali et a. 2010 (Mouse leukocytes)
Wilkie et al. 2010 (Rat skeletal muscle)
Korfali et a. 2012
(Rat liver; Rat leukocytes; Human muscle)
Cheng et al. 2019
(Mouse mesenchymal stem cells, adipocytes, myocytes)

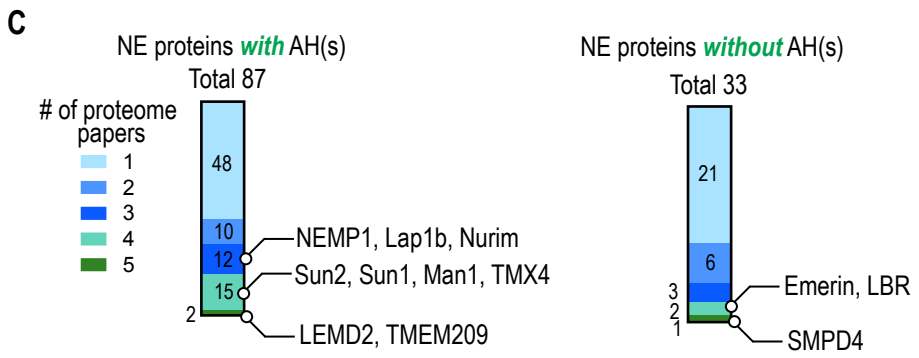
C
NE proteins with AH(s)
Total 87
# of proteome papers
1
2
3
4
5
48
10
12
15
2
NEMP1, Lap1b, Nurim
Sun2, Sun1, Man1, TMX4
LEMD2, TMEM209
NE proteins without AH(s)
Total 33
21
6
3
2
1
Emerin, LBR
SMPD4

Fig. S1. Computational screen of AHs in nuclear envelope proteins.

(A) Detailed flow chart of data mining for putative NE proteins and identification of predicted AHs. Numbers in parenthesis indicate the number of proteins. (B) Breakdown of the 410 NE proteins by the number of the NE proteome papers. NE proteins found in only a single NE proteome paper were further categorized by the specific NE proteome paper. (C) Breakdown of NE proteins with or without a predicted AH by the number of NE proteome papers.

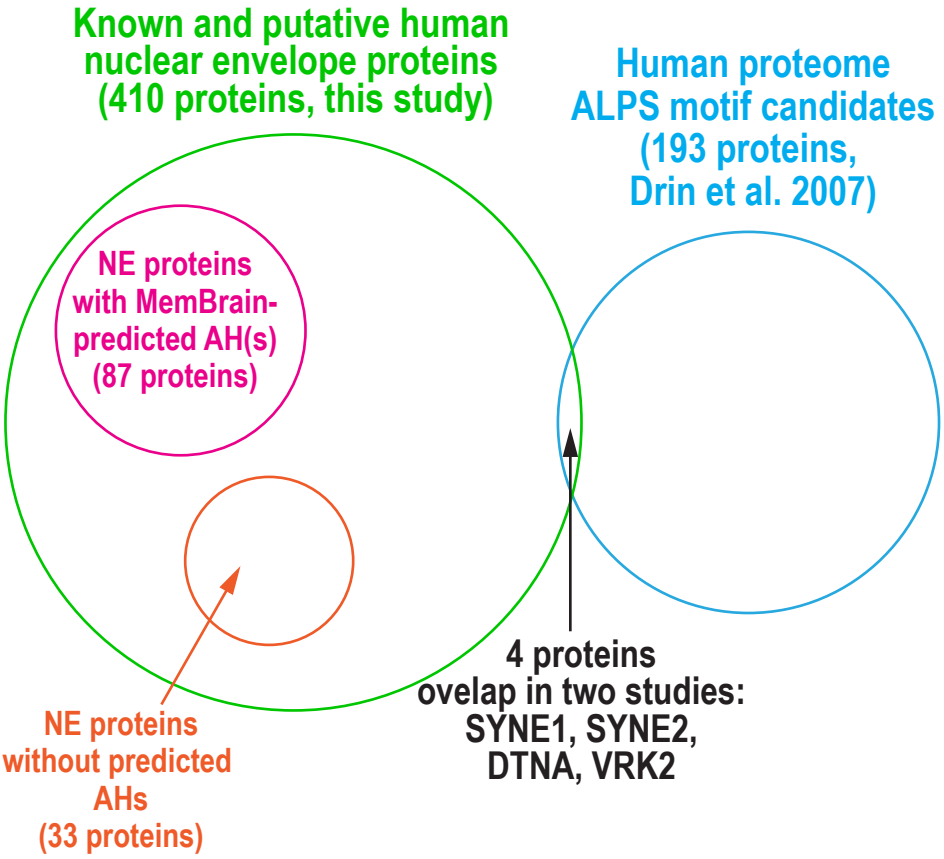
Known and putative human nuclear envelope proteins (410 proteins, this study)
Human proteome ALPS motif candidates (193 proteins, Drin et al. 2007)
NE proteins with MemBrain-predicted AH(s) (87 proteins)
NE proteins without predicted AHs (33 proteins)
4 proteins ovelap in two studies: SYNE1, SYNE2, DTNA, VRK2

Fig. S2. Overlap of AHs in this study and ALPS-like motifs in Drin et al. 2007.

Venn diagram representing the NE proteins, those with or without a MemBrain-predicted AH, and proteins with a putative ALPS-like motifs (Drin et al. 2007).

No membrane-bound organelle

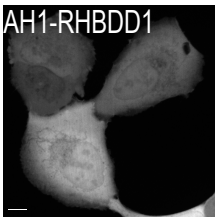

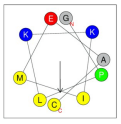

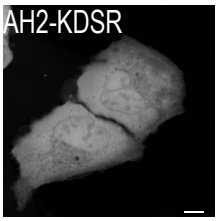

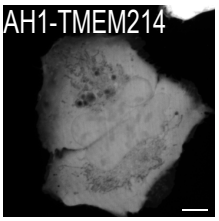

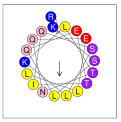

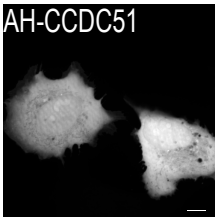

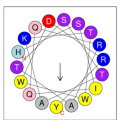

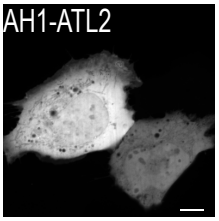

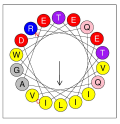

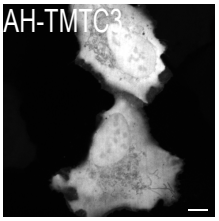

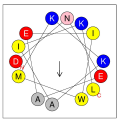

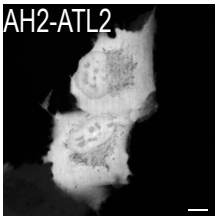

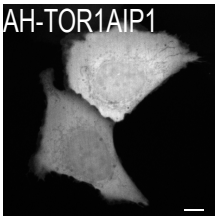

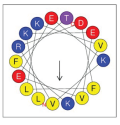

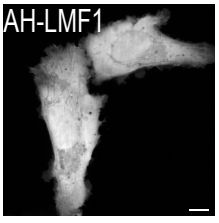

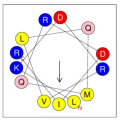

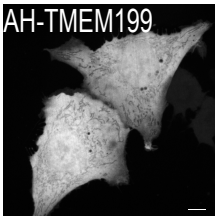

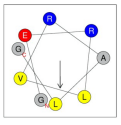

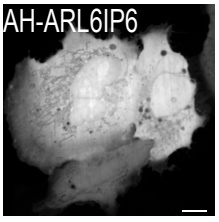

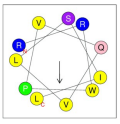

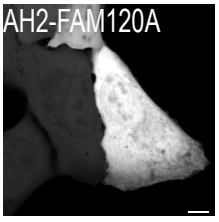

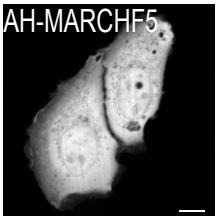

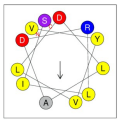

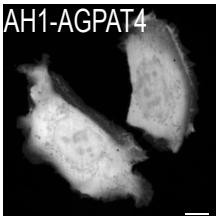

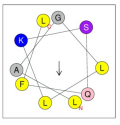

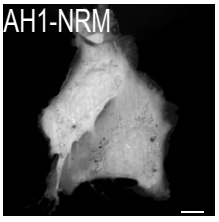

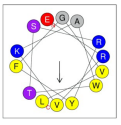

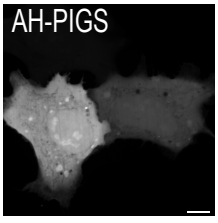

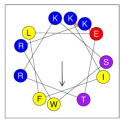

Nuclear bodies localized

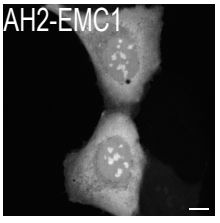

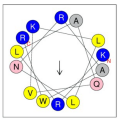

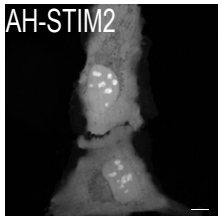

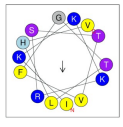

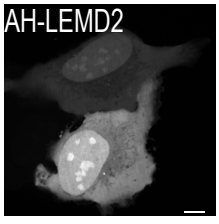

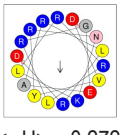

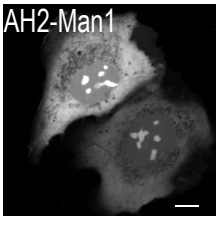

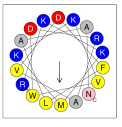

Fig. S3. Subcellular localization patterns of AH candidates tagged with mNG that did not localize to membrane-bound organelles.

Representative spinning disk confocal images of a single section in living U2OS cells expressing the indicated AH-mNG protein are shown. Schematic representations of corresponding helical wheel projections of the predicted AHs with mean hydrophobic moment <μH> and net charge z is shown. AH-mNG proteins with a nuclear body-like pattern are highlighted at the bottom right. Scale bars, 10 μm.

Lee et al. Supplementary Figure 4

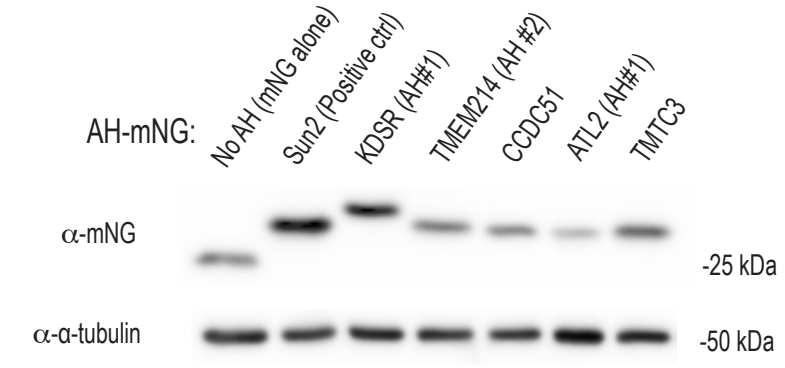

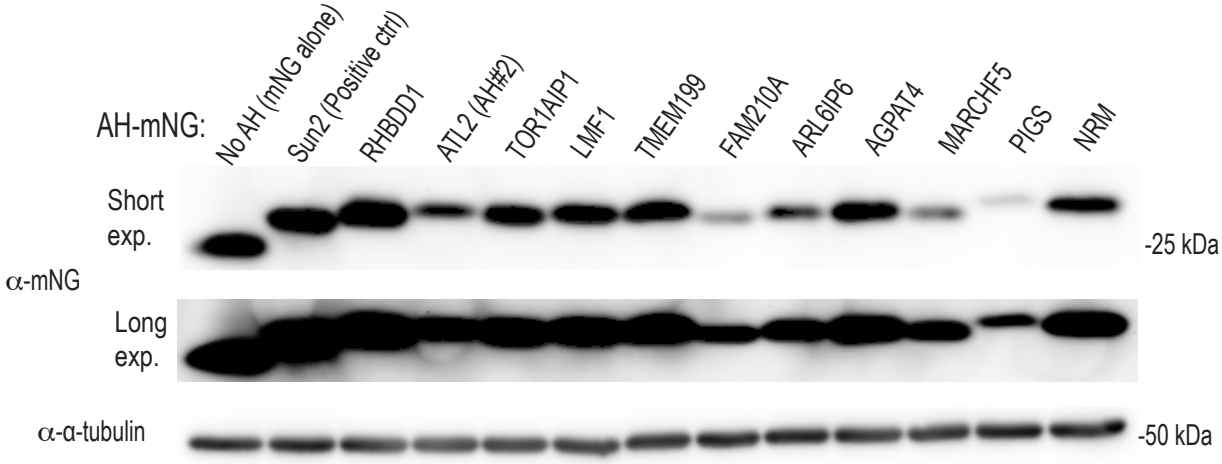

Fig. S4. AH-mNG without localization to membrane-bound organelles or nuclear bodies is expressed without unexpected cleavage of the AH.

Immunoblot of mNG alone or the indicated AH-mNG proteins transiently expressed in U2OS cells. Among the AH-mNG proteins without membrane-bound organelle localization (Fig. S2), we tested AH-mNG proteins that did not localize to nuclear bodies, because the nuclear body localization indicated the presence of AH in the expressed protein.

Golgi

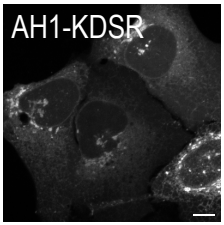

<μH> = 0.364
z = 0

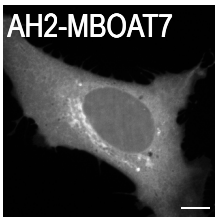

<μH> = 0.632
z = 0

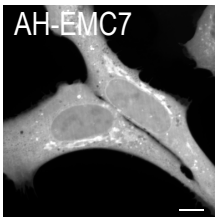

<μH> = 0.614
z = 0

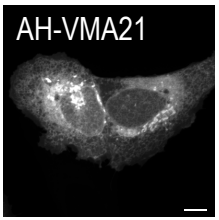

<μH> = 0.646
z = 1

ER/NE

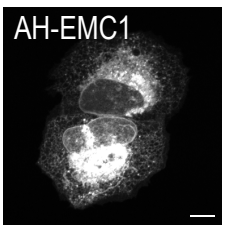

<μH> = 0.443
z = 3

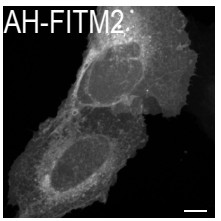

<μH> = 0.379
z = 3

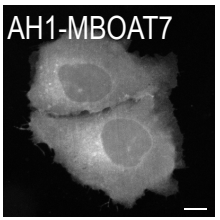

<μH> = 0.571
z = 3

ER/NE + Mitochondria

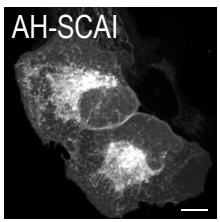

<μH> = 0.631
z = 2

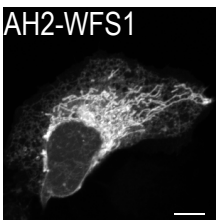

<μH> = 0.414
z = 0

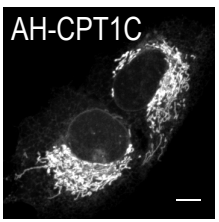

<μH> = 0.631
z = 2

Plasma membrane

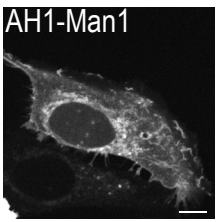

<μH> = 0.443
z = 4

Fig. S5. Subcellular localization patterns of AH candidates tagged with mNG that displayed non-mitochondrial patterns.

Representative spinning disk confocal images of a single section in living U2OS cells expressing the indicated AH-mNG protein are shown. Schematic representations of corresponding helical wheel projections of the predicted AHs with mean hydrophobic moment <μH> and net charge z is shown. Scale bars, 10 μm.

Lee et al. Supplementary Figure 6

Mitochondria

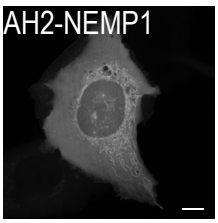

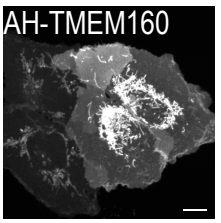

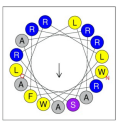

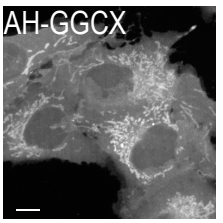

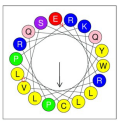

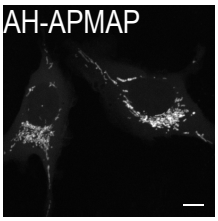

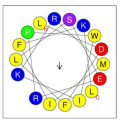

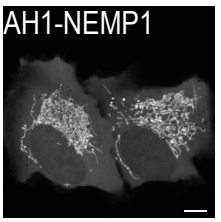

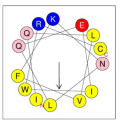

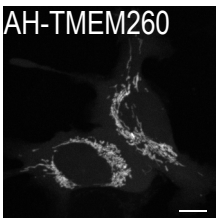

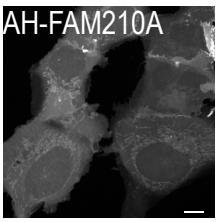

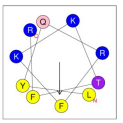

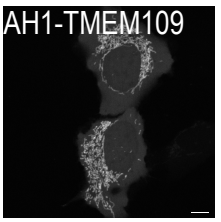

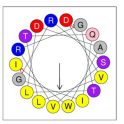

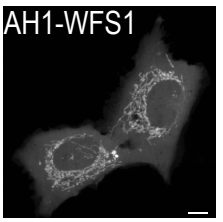

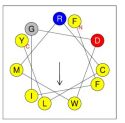

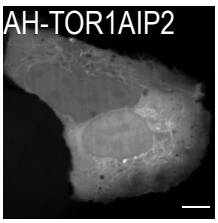

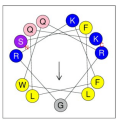

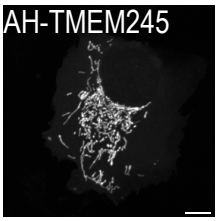

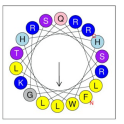

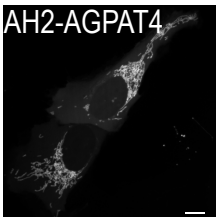

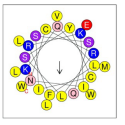

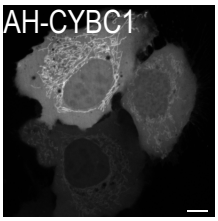

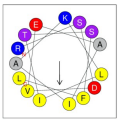

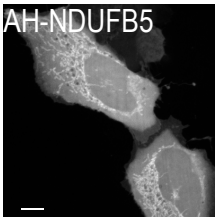

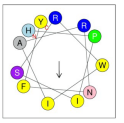

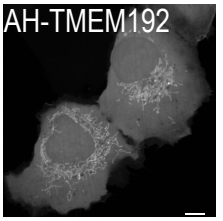

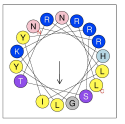

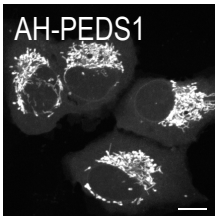

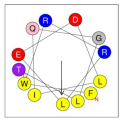

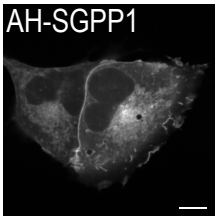

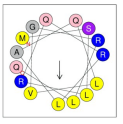

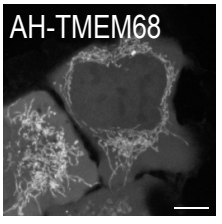

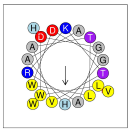

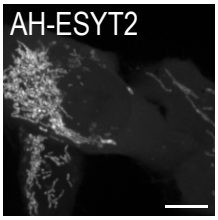

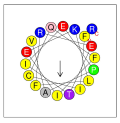

Fig. S6. Subcellular localization patterns of AH candidates tagged with mNG that displayed mitochondrial patterns.

Representative spinning disk confocal images of a single section in living U2OS cells expressing the indicated AH-mNG protein are shown. Schematic representations of corresponding helical wheel projections of the predicted AHs with mean hydrophobic moment <μH> and net charge z is shown. Scale bars, 10 μm.

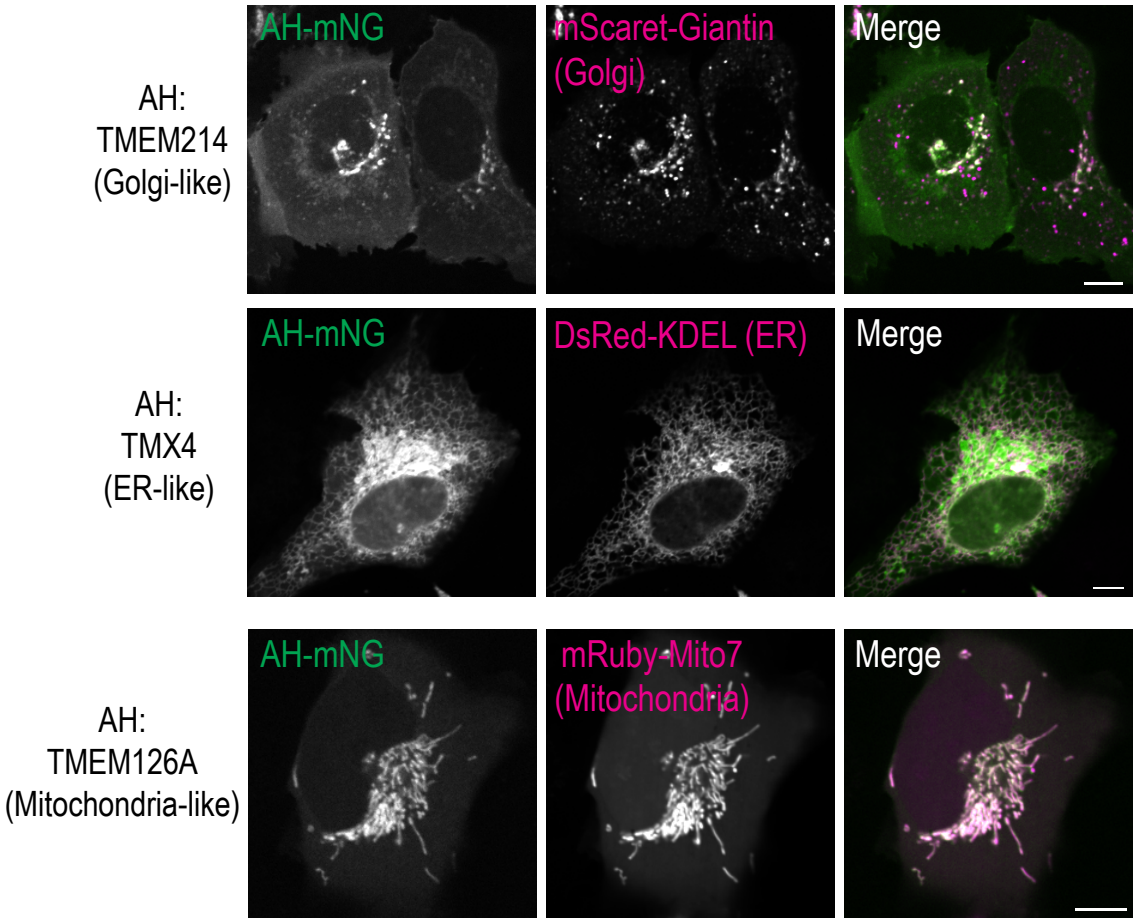
AH:
TMEM214
(Golgi-like)
AH-mNG
mScaret-Giantin
(Golgi)
Merge
AH:
TMX4
(ER-like)
AH-mNG
DsRed-KDEL (ER)
Merge
AH:
TMEM126A
(Mitochondria-like)
AH-mNG
mRuby-Mito7
(Mitochondria)
Merge

Fig. S7. Assessment of the organelle type to which that AH-mNG constructs localized.

Representative spinning disk confocal images of a single section in living U2OS cells co-expressing the indicated AH-mNG and the indicated organelle marker are shown. Scale bars, 10 μm.

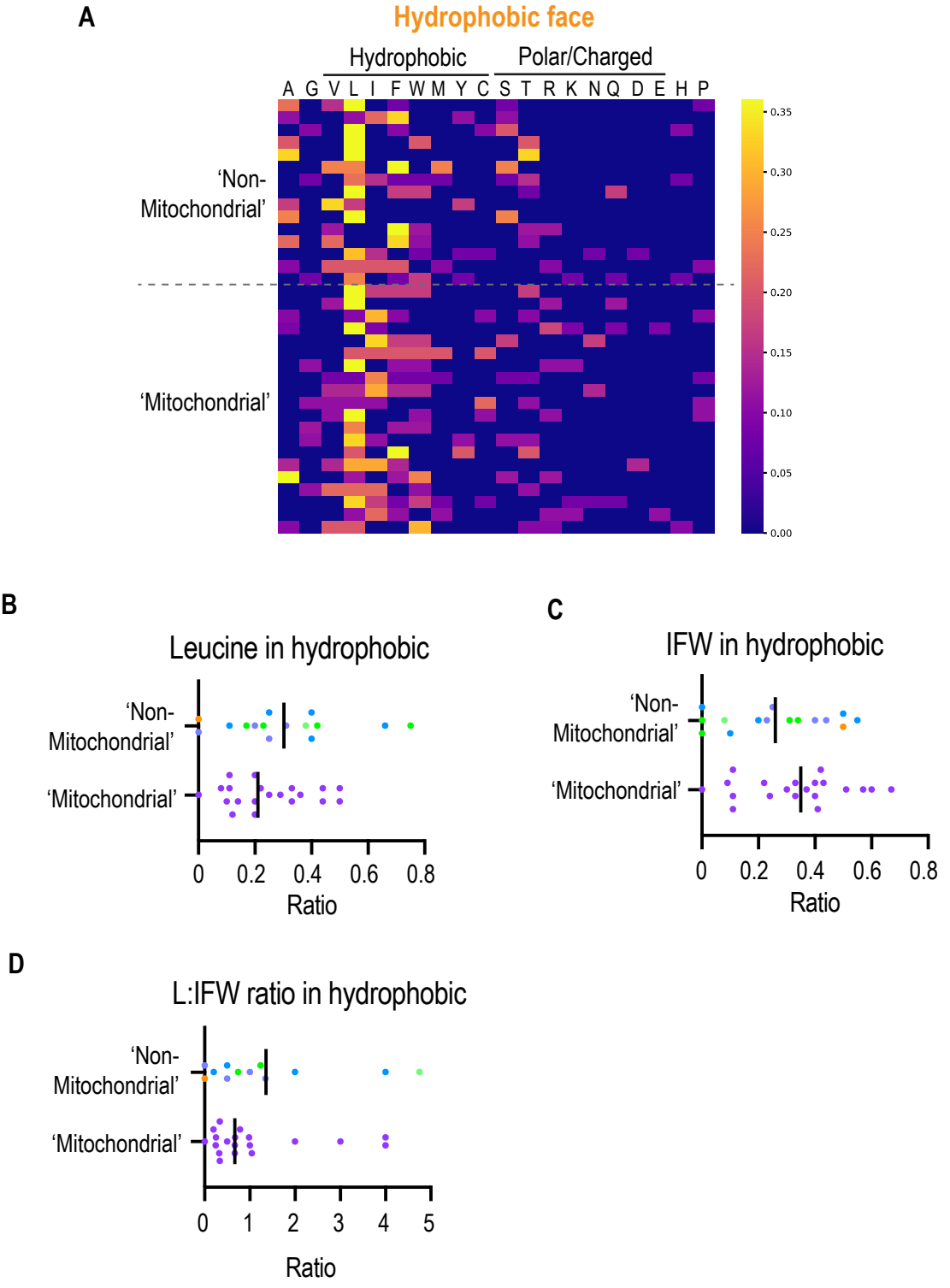
A
Hydrophobic face
Hydrophobic
Polar/Charged
A G V L I F W M Y C S T R K N Q D E H P
'Non-Mitochondrial'
'Mitochondrial'
0.35
0.30
0.25
0.20
0.15
0.10
0.05
0.00
B
Leucine in hydrophobic
'Non-Mitochondrial'
'Mitochondrial'
0 0.2 0.4 0.6 0.8
Ratio
C
IFW in hydrophobic
'Non-Mitochondrial'
'Mitochondrial'
0 0.2 0.4 0.6 0.8
Ratio
D
L:IFW ratio in hydrophobic
'Non-Mitochondrial'
'Mitochondrial'
0 1 2 3 4 5
Ratio

Fig. S8. Sequence codes in hydrophobic face that discriminate AHs with non-mitochondrial and mitochondria-like patterns.

(A) Heat map representation of the fraction of each amino acid (columns) present within the hydrophobic face of each amphipathic helix (row) categorized by indicated localization patterns. (B-D) Scatter plots of the indicated metrices of AH candidates categorized and color-coded by their localization patterns as determined from experiments in Fig. 1B.

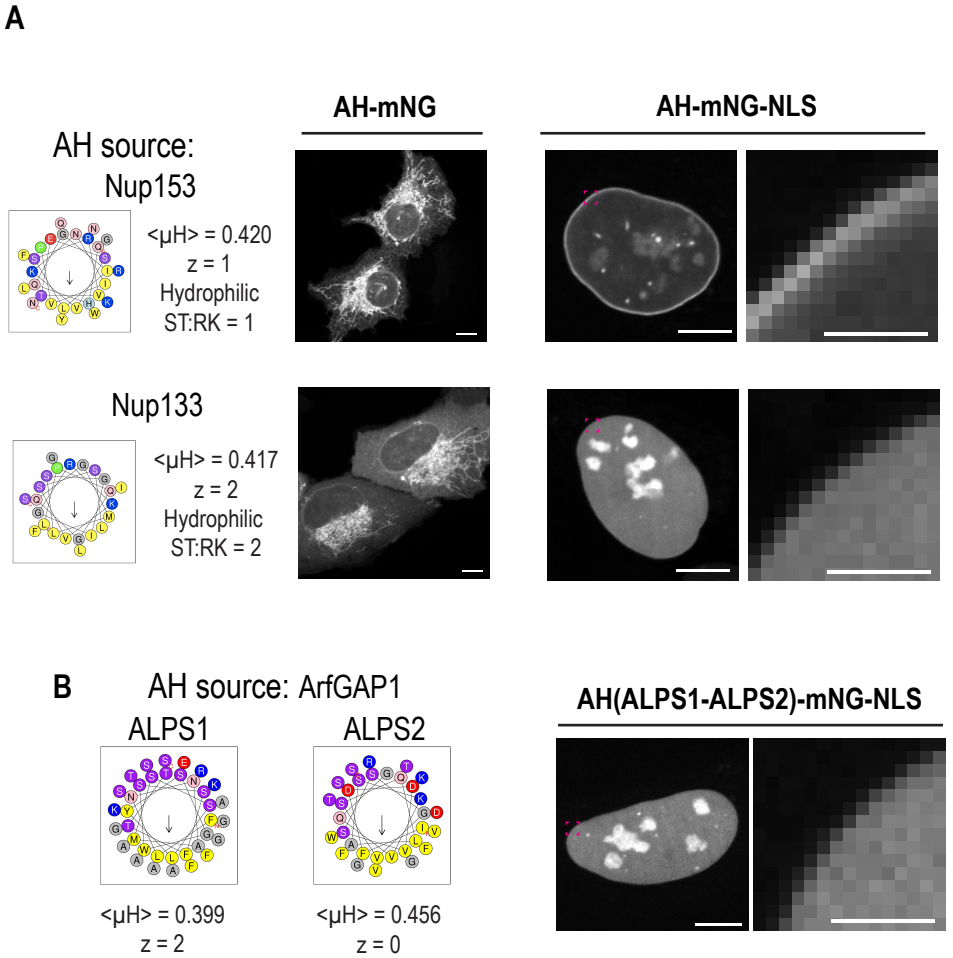
A
AH-mNG
AH-mNG-NLS
AH source:
Nup153
<μH> = 0.420
z = 1
Hydrophilic
ST:RK = 1
Nup133
<μH> = 0.417
z = 2
Hydrophilic
ST:RK = 2
B
AH source: ArfGAP1
ALPS1
ALPS2
<μH> = 0.399
z = 2
<μH> = 0.456
z = 0
AH(ALPS1-ALPS2)-mNG-NLS

Fig. S9. Subcellular localization patterns and INM association of AHs from human Nup153, Nup133 and ArfGAP1.

Representative spinning disk confocal images of a single section in living U2OS cells expressing the indicated AH-mNG (A) and AH-mNG-NLS protein with magnified zoom of the nuclear rim area (A and B) are shown. Schematic representations of corresponding helical wheel projections of the AHs with mean hydrophobic moment <μH> and net charge z is shown. Scale bars, 10 μm or 2 μm (zoom).

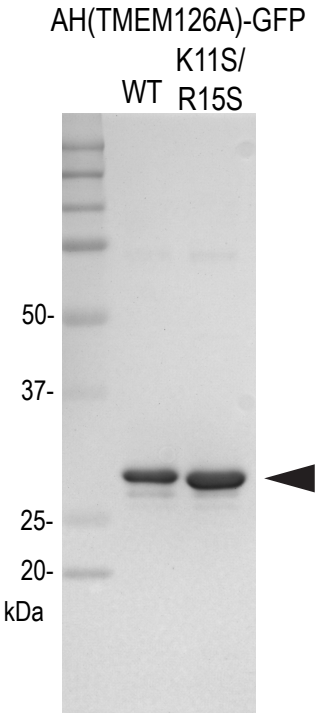
AH(TMEM126A)-GFP
WT
K11S/
R15S
50-
37-
25-
20-
kDa

Fig. S10. Purification of AH-GFP.

Coomassie staining of the indicated AH-GFP recombinant proteins expressed and purified from bacterial cells.

A

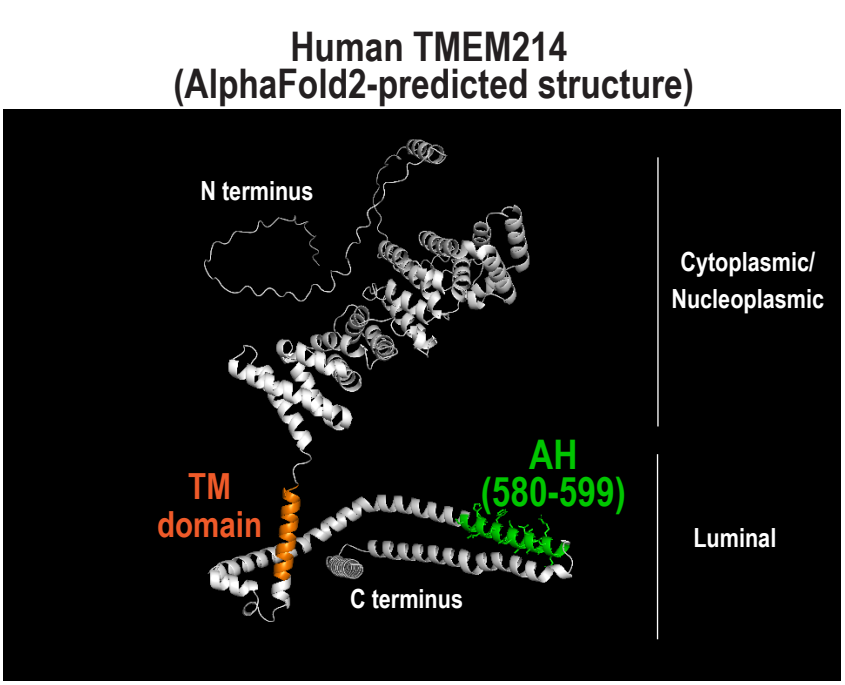
Human TMEM214
(AlphaFold2-predicted structure)
N terminus
Cytoplasmic/
Nucleoplasmic
AH
(580-599)
TM
domain
Luminal
C terminus

B

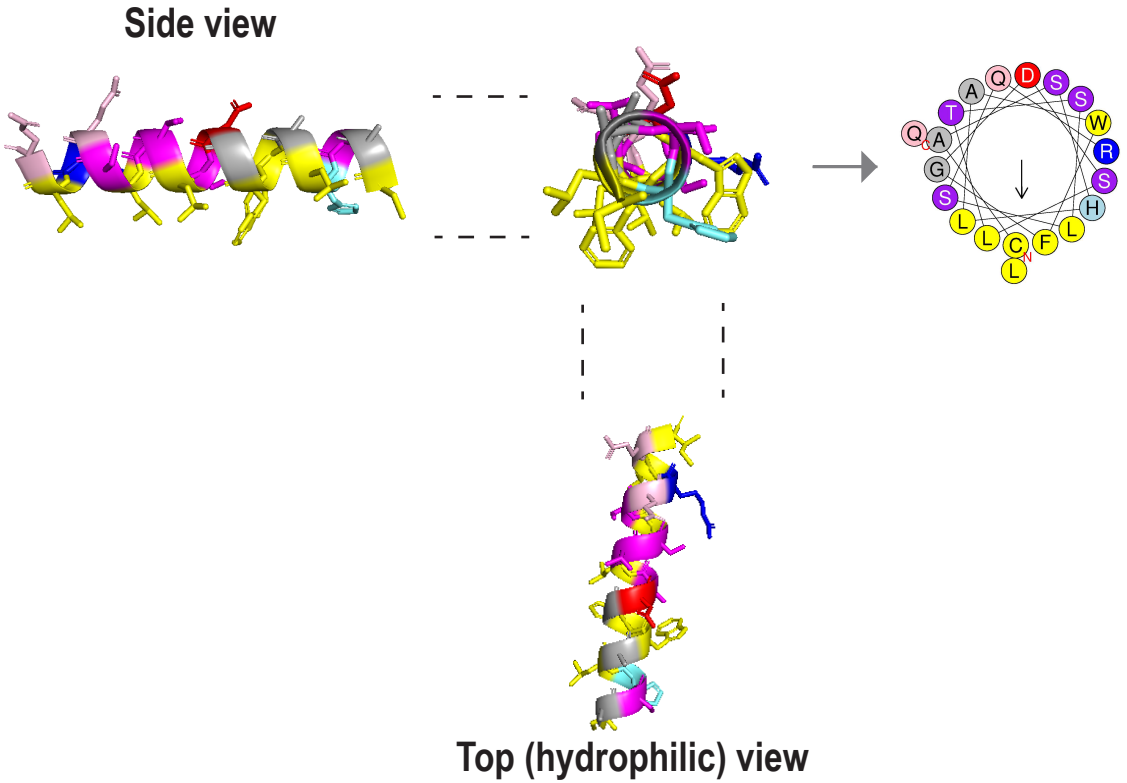
Side view
Top (hydrophilic) view

Fig. S11. Putative AH in TMEM214 protein.

(A) The putative AH is highlighted in the 3D structure of TMEM214 protein, predicted by AlphaFold2 and shown by PyMol. A putative transmembrane (TM) domain predicted by TMHMM is shown in brown. The N and C termini are predicted to face cytoplasm/nucleoplasm and NE/ER lumen, respectively, according to InterPro (ID: Q6NUQ4). (B) PyMol presentation of the TMEM214 AH. Amino acid residues are color-coded according to the wheel projection generated by HeliQuest.

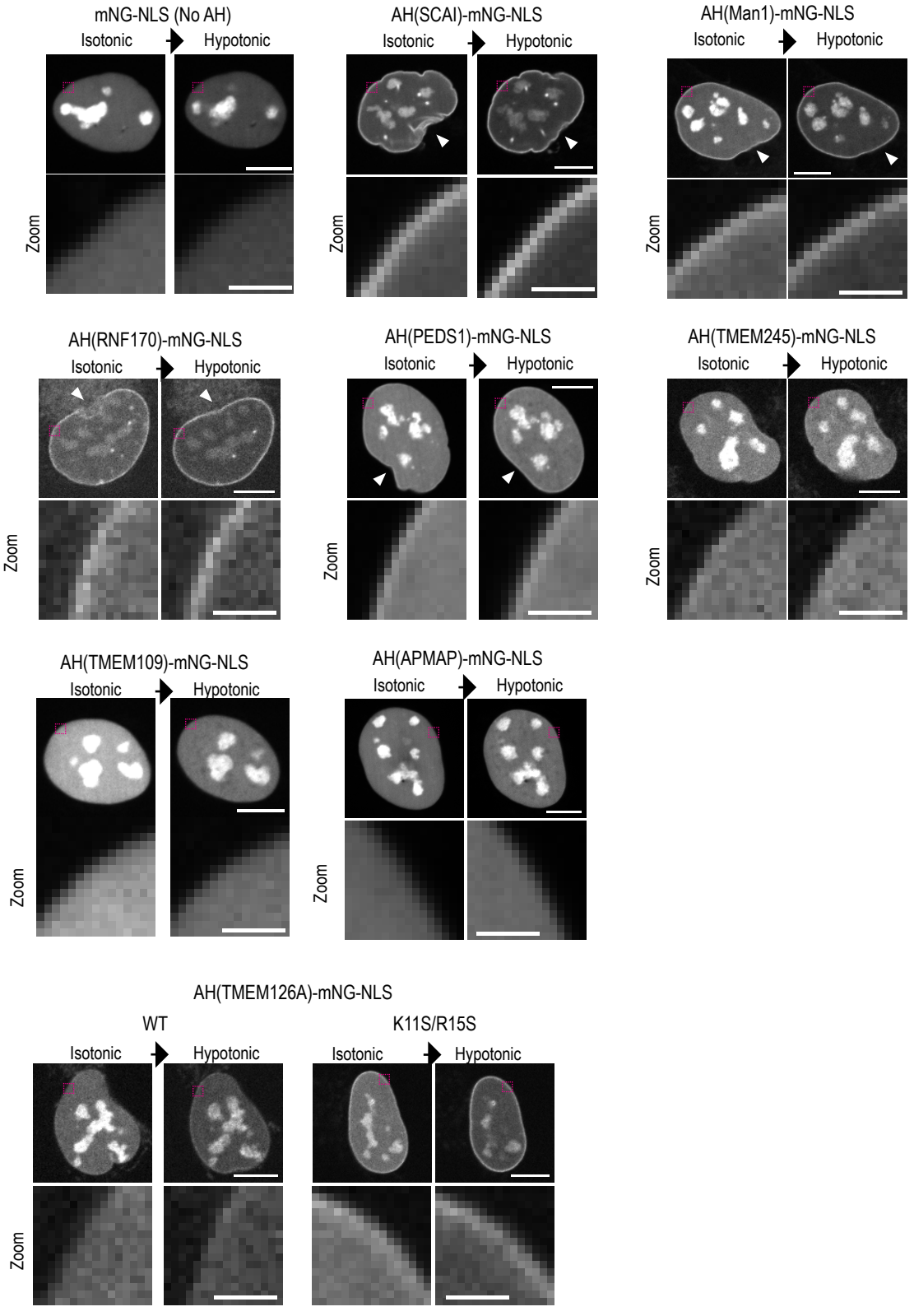
mNG-NLS (No AH)
Isotonic
Hypotonic
Zoom
AH(SCAI)-mNG-NLS
Isotonic
Hypotonic
Zoom
AH(Man1)-mNG-NLS
Isotonic
Hypotonic
Zoom
AH(RNF170)-mNG-NLS
Isotonic
Hypotonic
Zoom
AH(PEDS1)-mNG-NLS
Isotonic
Hypotonic
Zoom
AH(TMEM245)-mNG-NLS
Isotonic
Hypotonic
Zoom
AH(TMEM109)-mNG-NLS
Isotonic
Hypotonic
Zoom
AH(APMAP)-mNG-NLS
Isotonic
Hypotonic
Zoom
AH(TMEM126A)-mNG-NLS
WT
Isotonic
Hypotonic
Zoom
K11S/R15S
Isotonic
Hypotonic

Fig. S12. Hypotonic shock promotes AH binding to the inner nuclear membrane.

Single z-section spinning disk confocal images of living U2OS cells expressing with the indicated AH-mNG-NLS constructs before and after the hypotonic shock. An arrowhead indicates the deformation of the nuclear rim wrinkle that is no longer present after hypotonic shock. Scale bars, 10 µm or 2 µm (zoom).

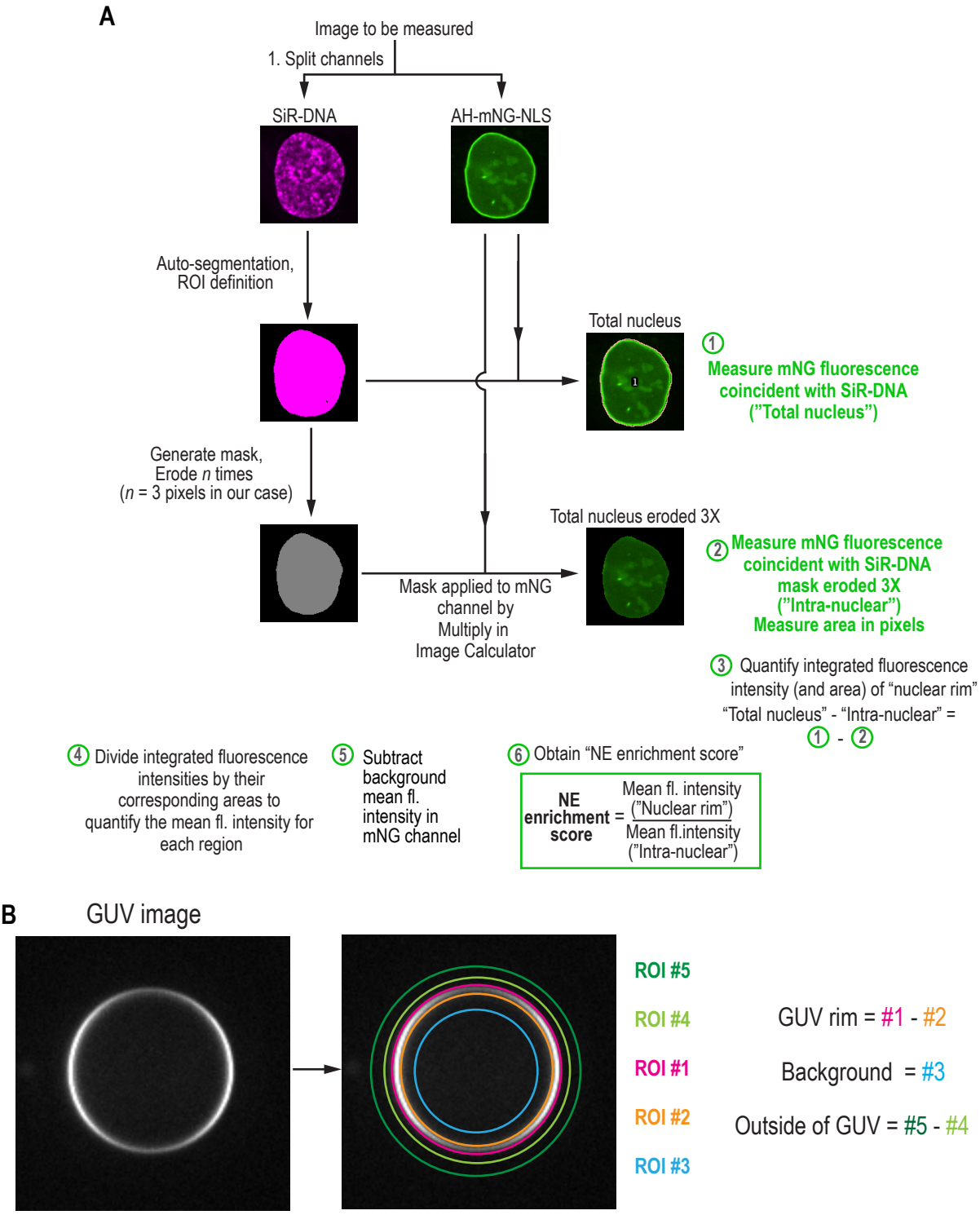
A
Image to be measured
1. Split channels
SiR-DNA
AH-mNG-NLS
Auto-segmentation,
ROI definition
Total nucleus
1
Measure mNG fluorescence
coincident with SiR-DNA
("Total nucleus")
Generate mask,
Erode n times
(n = 3 pixels in our case)
Total nucleus eroded 3X
2
Measure mNG fluorescence
coincident with SiR-DNA
mask eroded 3X
("Intra-nuclear")
Measure area in pixels
Mask applied to mNG
channel by
Multiply in
Image Calculator
3 Quantify integrated fluorescence
intensity (and area) of "nuclear rim"
"Total nucleus" - "Intra-nuclear" =
1 - 2
4 Divide integrated fluorescence
intensities by their
corresponding areas to
quantify the mean fl. intensity for
each region
5 Subtract
background
mean fl.
intensity in
mNG channel
6 Obtain "NE enrichment score"
NE enrichment score = Mean fl. intensity ("Nuclear rim") / Mean fl.intensity ("Intra-nuclear")
B
GUV image
ROI #5
ROI #4
ROI #1
ROI #2
ROI #3
GUV rim = #1 - #2
Background = #3
Outside of GUV = #5 - #4

Fig. S13. Flow chart of the NE enrichment score quantification and schematic of ROIs in AH-GUV binding quantification.

(A) Flow chart of the NE enrichment score quantification. (B) Schematic illustration of ROIs in AH-GUV binding quantification. See methods for more detail.